

Supporting online information for:

Climate Change Impact of Biochar Cook Stoves in Western Kenyan Farm Households: System Dynamics Model Analysis

THEA WHITMAN¹, CHARLES F. NICHOLSON², DORISEL TORRES¹, AND JOHANNES LEHMANN^{1*}

* Corresponding author email: CL273@cornell.edu, phone: (607) 254-1236

¹Department of Crop and Soil Science, Cornell University, Bradfield Hall, Ithaca NY, 14853, USA

²Department of Agribusiness, California Polytechnic State University, San Luis Obispo, CA 93407

This SI document includes text, tables, and figures with detail on the model development, simulations, and evaluation.

Topic	Page
1. Study System Location	S2
2. Model Module Overview	S3
3. On-Farm Biomass Production	S3
4. Fuel Use and Emissions	S8
5. Soil Carbon	S11
6. GHG Impact	S14
7. Model Scenario Design	S16
8. Model Evaluation	S17
9. Further GHG Impact Results	S21
10. Further Soil Carbon Results	S21
11. Further Sensitivity Analysis Results	S24
12. Policy Analysis Results	S25
13. Literature Cited	S28

1. Study System Location

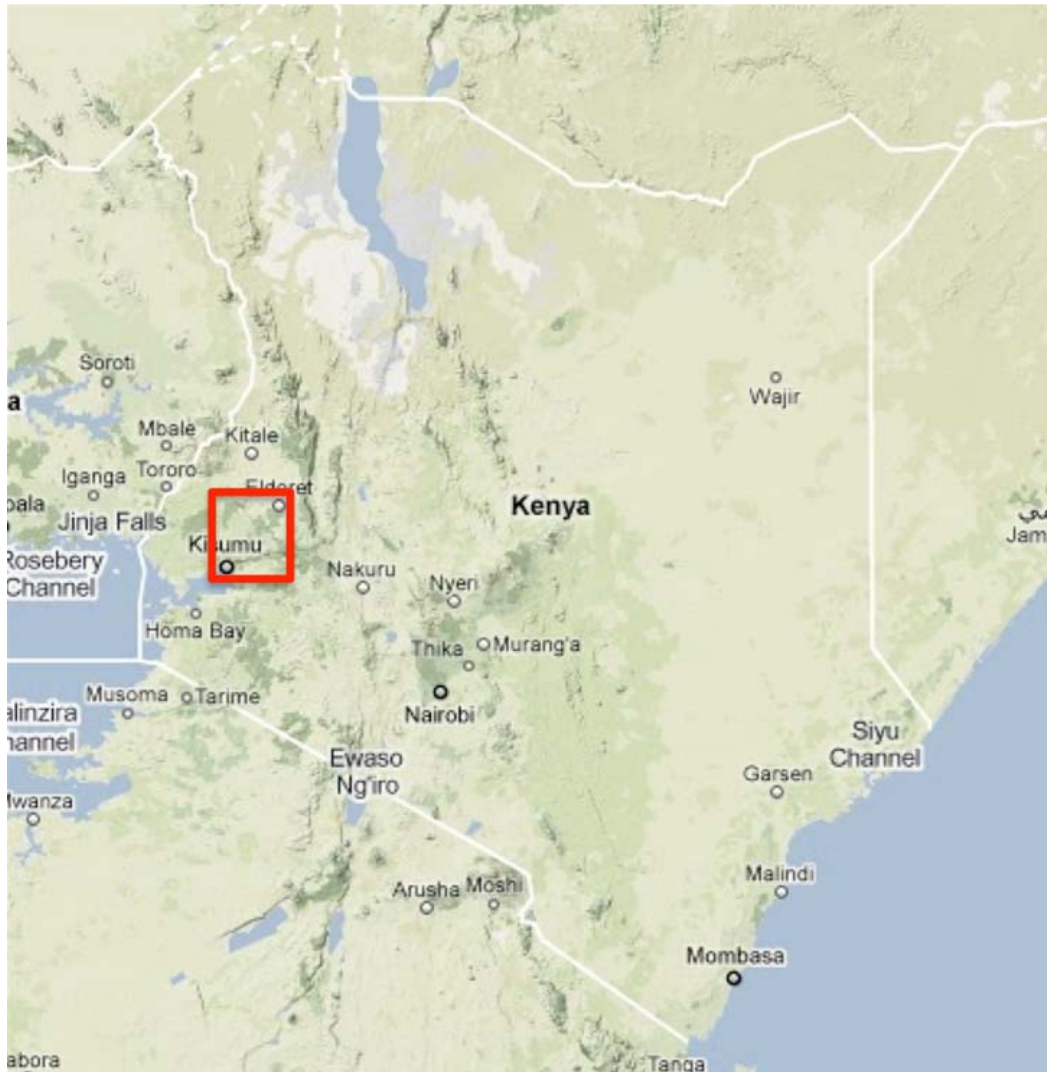


FIGURE S1. Studied region in the western Kenyan highlands indicated in rectangle. Map from Google maps (maps.google.com).

2. Model Module Overview

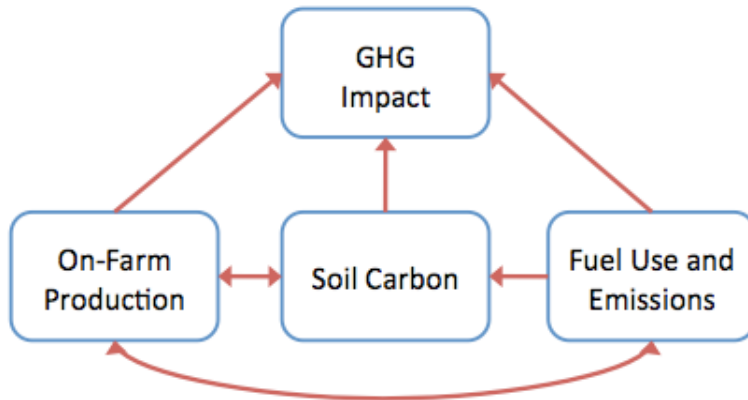


FIGURE S2. Model modules and their interconnections.

3. On-farm biomass production

An overview of the on-farm biomass production module is illustrated in Figure S3.

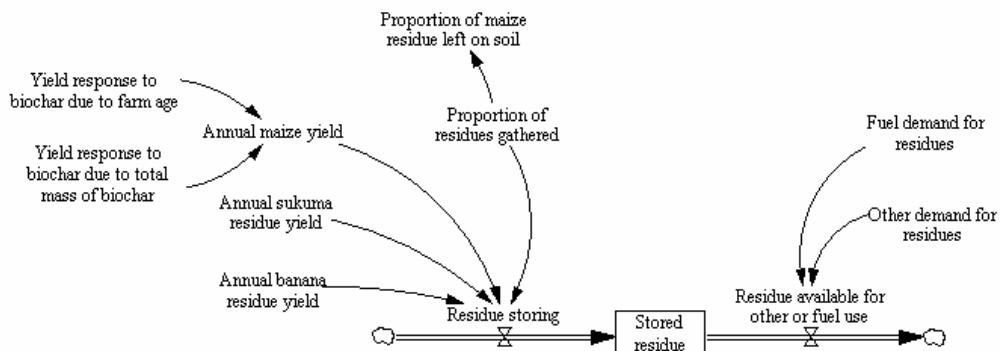


FIGURE S3. Overview of on-farm biomass production module.

The annual maize stover yield is calculated based on mean yields for short and long rains.

Maize grain yields for the long-rains season (March-May) are based on the mean values from farm plots amended with only K and P (100 kg/ha/year for each), from seasons 2004-2009 and decline with increasing time since farm conversion from forest (Figure

S4). Limited data are available (2004 only) for the short rain season (October and November), so the mean value across conversion years, 2.4 t dry grain/ha, is used [1]. Data from field surveys of 60 farmers indicated that around 25% of stover is currently used for other uses, such as lighting fires or feed for animals, while 75% is left on the field.

To predict cob yield, a linear equation relating the ratio of cob:grain mass yield per hectare to farm age was fitted for the cob and grain mass data collected, giving cob:grain ratio = $0.3613 + 0.002 * [\text{conversion year}]$, or, if data from the year 2009, which was a severe drought year, are included, cob:grain ratio = $0.0057 + 0.3049 * [\text{conversion year}]$. Cobs are commonly used to light fires, and while they could feasibly be used as fuel in a pyrolytic stove, it is assumed that they would continue to be used for lighting fires, and thus are not included as an additional biomass source.

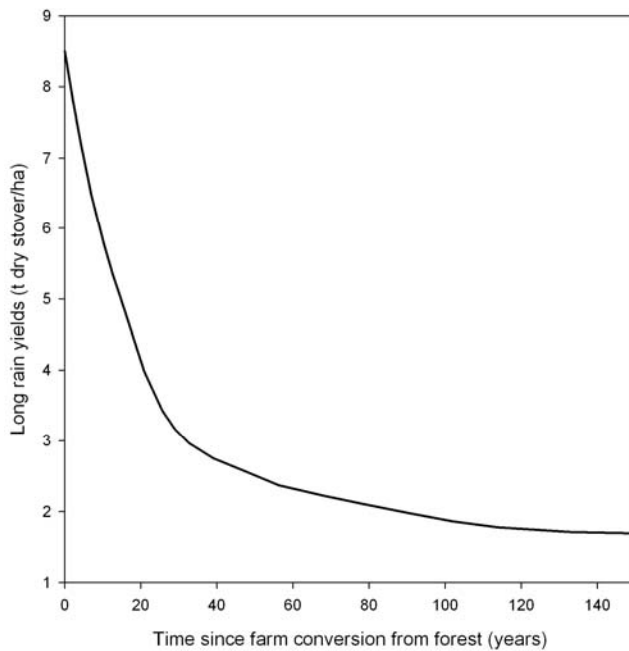


FIGURE S4. Long rain maize stover yield over time, based on 2004-2009 chronosequence data.

The magnitude of the crop's response to biochar application is based on the age of the farm and the total biochar that remains on the soil, as shown in Equation 1,

$$Y_{A,BC} = Y_B \cdot I_{max} \cdot \left(E_{BCA} \left(\frac{A_F}{A_{Fmax}} \right) \right) \cdot \left(E_{BCS} \left(\frac{S_{BC}}{S_{BCmax}} \right) \right) \quad (1)$$

where $Y_{A,BC}$ is crop yield in t dry grain/ha for a farm at a given age (A) and soil biochar content (BC), Y_B is the baseline yield in t/ha, I_{max} is the maximum increase factor (2.2, or 116%, based on the mean increase in yields observed at 18 t C/ha biochar application from Kimetu [2], A_F is the age of the farm and A_{Fmax} is the age of a farm above which the maximum benefit is garnered (set at 100 years), S_{BC} is the stock of all biochar in the soil, S_{BCmax} is the stock of biochar above which the maximum benefit is realized (estimated at 25 t/ha), E_{BCA} is the degree of effect from biochar due to age, a value between 0-1 which increases rapidly over between 0-15 years, after which it increases more slowly (Figure S5), and E_{BCS} is the degree of effect from biochar due to the total stock of biochar in the soil, also a value between 0-1, which increases steadily as the mass of biochar increases (Figure S6). The two E functions serve to determine the degree to which the possible percent yield increase is realized. If either has a value of 0, there will be no effect, and if both have a value of 1, then the full impact on yields, I_{max} , will occur. This response is analogous to N and P fertilizer response curves for these farms [1] (although biochar would not be expected to use the same mechanisms as fertilizers to increase yields).

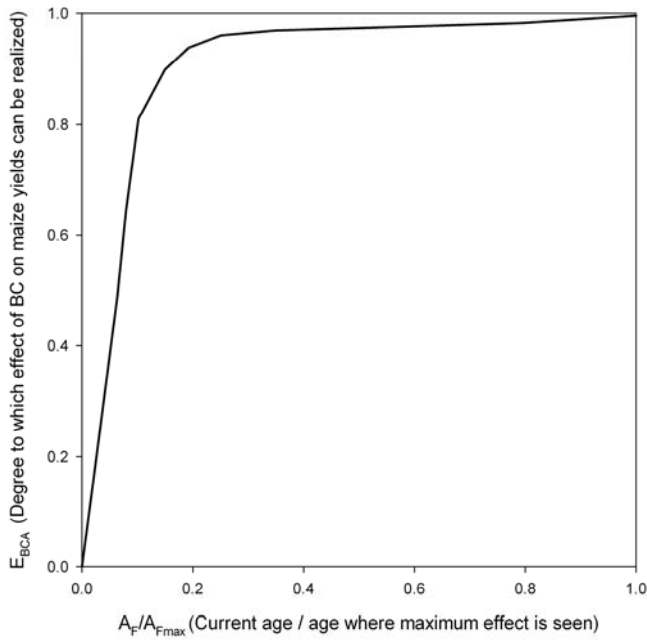


FIGURE S5. Function indicating how farm age affects the degree to which the full effect of biochar on maize yields is realized.

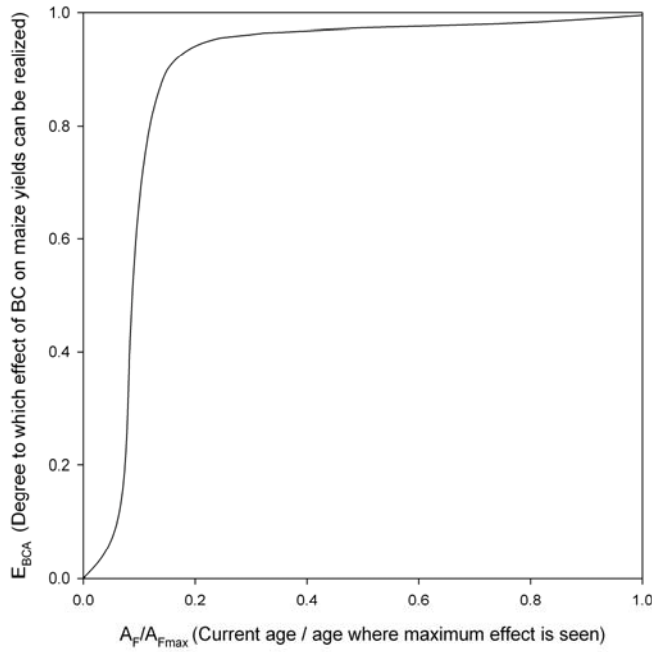


FIGURE S6. Function indicating how biochar mass affects the degree to which the full effect of biochar on maize yields is realized.

The studied farm chronosequence shows a decline in soil C, N, and fertility over time [2, 3], because of the specific practices applied to the fields and other land-use decisions. Thus, while farm age is used as a proxy for soil degradation over time in this model, the relationship of GHG reductions to age would not be directly transferrable to different systems, but the different results on soils of different fertility statuses would be more transferrable, as has been established for farm gradients [4].

Production of banana leaves and *sukuma-wiki* clippings represent residues that are currently unused on the farm, and were derived from on-farm biomass surveys conducted in 2008 by Torres [5]. No consistent trend in yield was seen by conversion year, so the mean farm area devoted to each crop and the mean annual yield per hectare are used to calculate total available biomass (Table S1). Production of on-farm wood represents the mean annual incremental (MAI) growth of on-farm trees, and was derived from on-farm biomass surveys conducted by Torres in 2008 [5]. No consistent trend in MAI was seen by conversion year, so the mean farm area devoted to trees and the MAI per hectare across all farms are used to calculate total available biomass (Table S1).

TABLE S1. On-farm Biomass Production

Biomass	Area devoted to crop (ha)	Mean annual available yield (t C/ha)
Banana	0.052	7.6
<i>Sukuma-wiki</i>	0.018	1.3
Wood	0.223	4.7

4. Fuel Use and Emissions

An overview of the fuel use and emissions module is illustrated in Figure S7.

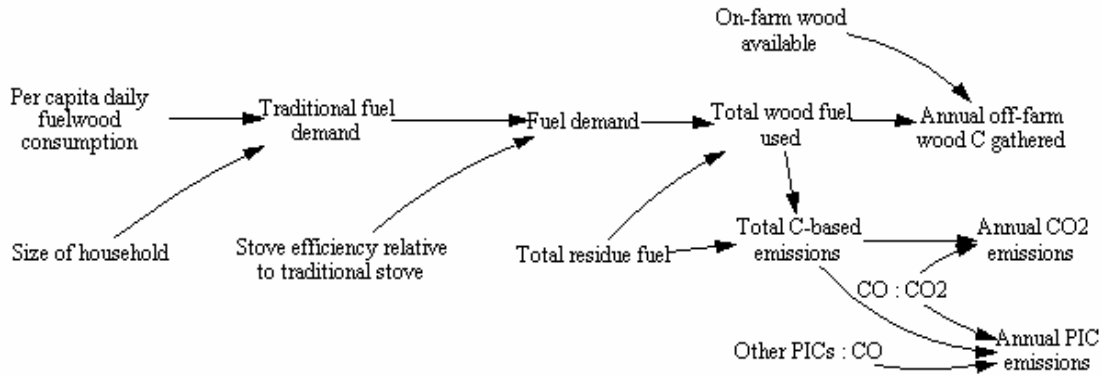


FIGURE S7. Overview of fuel use and emissions module.

Daily per-capita fuel use was calculated over 3-5 days in July 2009, using a Kitchen Performance Test (KPT) in 17 homes, 6 of which use 3-stone cook stoves, and 11 of which use modified mud cook stoves (locally referred to as Chepkube stoves). Fuel samples were taken at each weighing to determine moisture content, which was calculated as proportion of mass lost after heating to 70°C for over 48 hours, until constant mass was reached. The mean fuel use was 1.9 ± 1.1 kg dry wood/capita/day for the 3-stone cook stove, and 1.4 ± 0.7 kg dry wood/capita/day for the Chepkube stove. The value of 1.9 kg dry wood/capita/day was used in the model for the 3-stone cook stove baseline, but was subjected to sensitivity analyses that reflect the range of values observed. Relative stove fuel use was determined as described in the main manuscript and in Table S2.

TABLE S2. Modelled Stove Parameters

Stove type	Fuel use (kg dry biomass / capita / day)	CO:CO₂ ratio by mass C
3-Stone	1.95 ^a	0.0513 ^d
Rocket stove	0.72 ^b	0.0155 ^e
Pyrolysis stove	1.24 primary + 0.84 secondary (prototype); 1.022 primary + 0.70 secondary (refined) ^c	0.0252 ^f

a. Measured using kitchen performance tests [6]; b. Calculated using measured fuel use for the system and the fuel use ratio of 3-stone to rocket stove [7]; c. Primary biomass is used to light the stove, while secondary biomass represents that which is pyrolysed. Values are from [5] and [7]; d. Mean value from high and low power water boiling tests (WBTs) from MacCarty et al. [7], Jetter and Kariher [8], and in-home cooking tests from Johnson et al. [9]; e. Mean value of high and low-power WBTs of the rocket stoves in MacCarty et al. [7] and Jetter and Kariher [8]; f. Gasification stove value in MacCarty et al [7]

For calculating per-capita fuel use from the KPT, capita values are adjusted to a standardized unit: men over 14 years of age are weighted at 1.0, men over 59 at 0.8, women over 14 at 0.8, and children 14 and under at 0.5 [6].

For the pyrolysis stove, 59.5% of the C is retained in the biochar (mean measured for sawdust, maize cobs, and maize stover feedstocks from Torres [5]). Division of the remaining C between CO₂ and PICs is based on the relative ratios of these products. The CO:CO₂ ratio is a common metric for determining how efficient combustion of fuel is: a high ratio results from low-efficiency combustion with high PIC production (Table S2). This ratio was calculated for a range of different stoves. Here, we use the mean value from high and low power water boiling tests (WBTs) [7, 8], and in-home cooking tests

[9] for the 3-stone stove. Whether stoves are used at higher or lower power is determined by home-specific cooking activities, and the balance can be important in determining CO:CO₂ ratios, which, in turn, will influence stove GHG production, as illustrated by Johnson et al. [9]. The value used for the pyrolysis stove is based on the gasification stove measured in [7] and is in the mid-range of values calculated for improved cook stoves that do not use charcoal as fuel as measured by [8]. The CO:CO₂ ratio used for the rocket cook stove is taken from the mean value of high and low-power WBTs of the rocket stoves in [7] and [8]. We model the emissions of non-CO PICs as being proportional to CO emissions, based on ratios from [7, 9, 10], and [11] for CH₄ (0.063) and from [9] and [12] for black C (0.00011) and non-black aerosol C (0.042). Using these ratios, we divide the total C lost from the fuel during combustion among the four end products using eq. 2 to determine the mass of CO₂ released and the ratios above to determine the mass of the other C-based compounds released,

$$CO_2 = \frac{C_E}{X_{CO_2} + (CO:CO_2)[X_{CO} + (CH_4:CO) \cdot X_{CH_4} + (EC:CO) \cdot X_{EC} + (OC:CO) \cdot X_{OC}]} \quad (2)$$

where X_Y is the molar mass ratio of carbon to compound Y and C_E represents the total mass of C emitted from the stove.

5. Soil Carbon

An overview of the soil carbon module is illustrated in Figure S8.

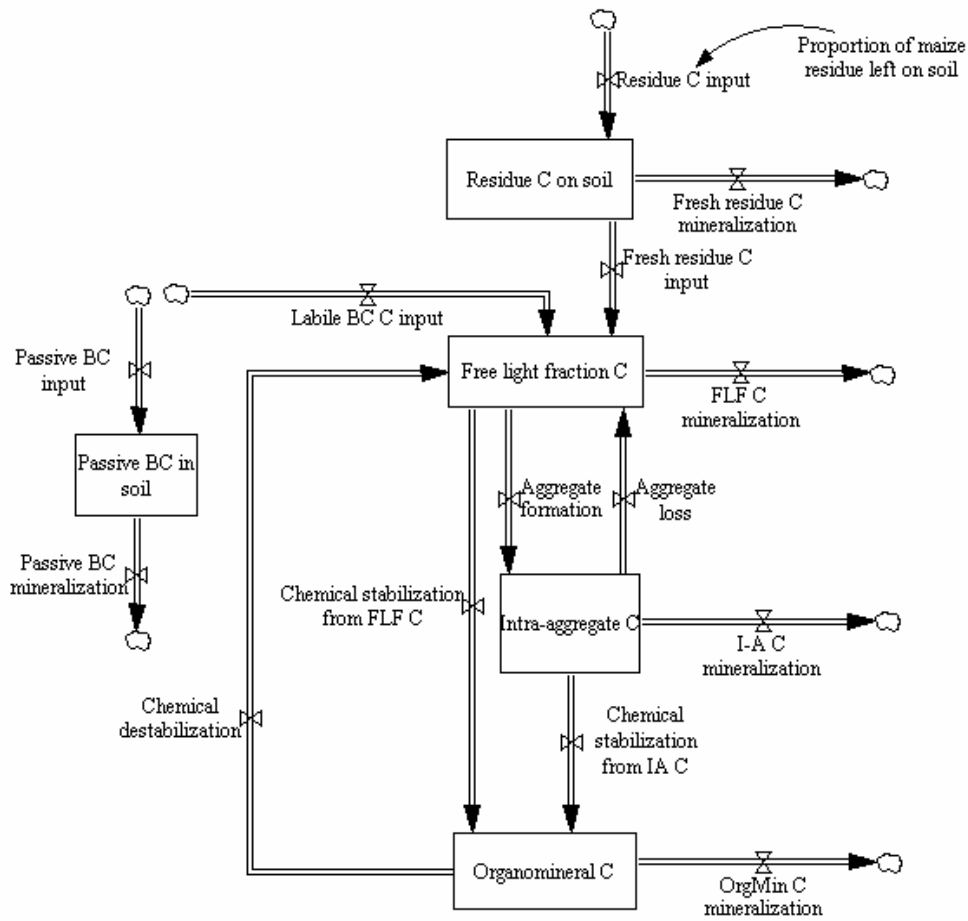


FIGURE S8. Overview of soil carbon module.

The soil C module was parameterized by fitting turnover time parameters for C pools so that with the measured maize stover inputs of farms of different ages providing the residue input, modeled SOC pool sizes corresponded to the measured soil C stocks, under the designed model structure (Table S3).

TABLE S3. Soil Carbon Parameters after Calibration

Pool	Initial C stock when $A_{initial}=1$ (tC/ha)	Turnover time (years)	Fraction mineralized (%)
Residue C	labile – 2.25 recalcitrant - 0.75	labile - 1 recalcitrant - 10	45
Free light C	15.85	1.75	45
Intra-aggregate C	6.525	1.83	55
Organomineral C	27.58	57.67	55

This resulted in simulation outcomes that compare well with experimental data, as shown in Figure S9.

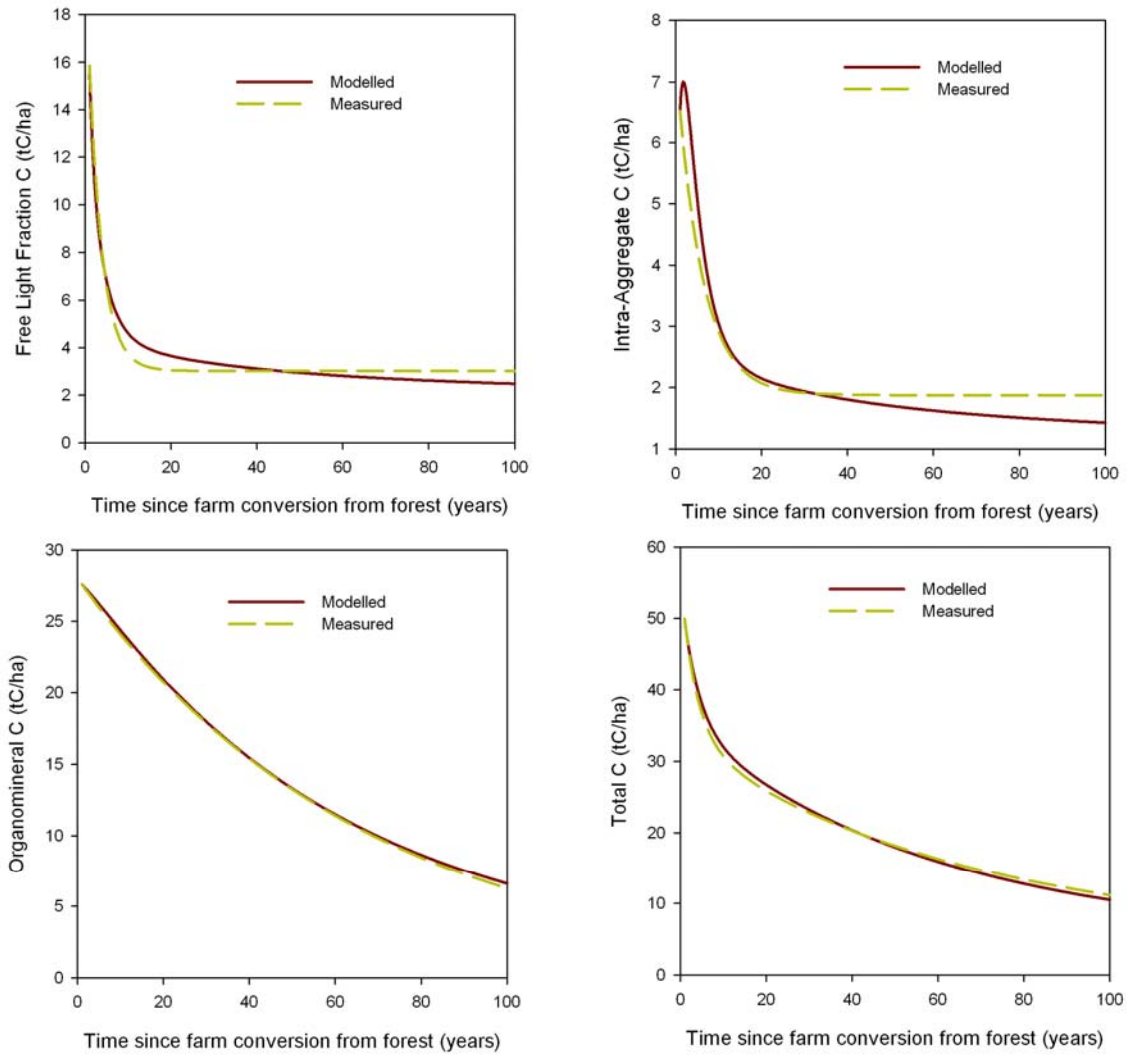


FIGURE S9. Measured and modeled SOC pools after model parameterization.

6. GHG Impact

Characteristics of GHGs are listed in Table S4.

TABLE S4. GHG Characteristics

Gas	GWP	rGWP	Kyoto Status
CO ₂	1 ^a	0	Included
CH ₄	25 ^a	22	Included
CO	1.9 ^a	0.3	Not included
EC	597 ^b	593	Not included
OC	0, but likely negative ^c	0, but likely negative	Not included

a. [13] b. [14-16] c. [17];

In general, any decrease in gaseous stove emissions produces a decrease in net GHG impact, W , while any increase in terrestrial C storage results in a decrease in W . The net change, ΔW_i , for a given stove, i , is calculated as shown (eq. 3),

$$\Delta W_i = (W a_i - W a_{3\text{-stone}}) - (W t_i - W t_{3\text{-stone}}) \quad (3)$$

where $W t_i$ represents net terrestrial GHG impact for a given stove, i , and $W a_i$ represents net atmospheric GHG impact for a given stove, i . $W t$ and $W a$ are calculated differently for each biomass type, depending on whether all its C flows are included within the model boundary, as with maize stover (m), or whether its C flows are modeled, in part, indirectly and it is either non-renewable (n) or renewable (r), as these terms are defined in the paper.

We calculate the net GHG impact of released gases in terms of CO₂e, $W a_i$ for a given stove, I , as (eq. 4)

$$Wa_i = \sum_k ([G_{imk} + G_{ink}] \cdot GWP_k) + \sum_k (G_{irk} \cdot rGWP_k) + WaBC_{in} \quad (4)$$

where G_{imk} , G_{ink} , and G_{irk} represent the net gaseous emissions of GHG k , from either maize, non-renewable, or renewable fuel sources, respectively; GWP_k and $rGWP_k$ are the GWP and renewable GWP, respectively, of GHG k ; and $WaBC_{in}$ represents the CO₂ released from the mineralization of biochar produced from non-renewable biomass source n .

We calculate the net GHG impact of terrestrial C storage in terms of CO₂e, Wt_i , for a given stove, I , as (eq. 5)

$$Wt_i = (SOC_{im} + Cr_{im} + BC_{im} + BC_{ir}) \cdot M_{CO_2} \cdot GWP_{CO_2} \quad (5)$$

where SOC_{jm} is the total mass of SOC in the soil from maize stover; Cr_{im} is C in gathered and stored maize stover; BC_{jm} and BC_{jr} are the total mass of C in biochar in the soil that was created from maize stover and renewable biomass, respectively; M_{CO_2} is the molar mass ratio of CO₂ to C; GWP_{CO_2} is the GWP of CO₂. Equations 4 and 5 are used to solve eq. 3 for each different stove, I .

Recall that mineralization of biochar produced from non-renewable sources is considered to be a net release of C to the atmosphere and that C stored in biochar produced from renewable sources is considered to be a net withdrawal from the atmosphere, as elaborated on in the paper. We note that by excluding BC_{in} , we are assigning it an effective value of 0 – that is, as discussed in the paper, biochar produced from non-renewable biomass sources does not provide any net C storage. However, one could take the non-renewable or unsustainable scenario a step further and account for the loss of

root, leaf, and soil C that are associated with the loss of wood during deforestation, which would require that we assign a negative value to BC_{in} . We have not taken this approach, recognizing that the fNRB is an abstraction to begin with and noting that an ideal solution would be to measure and model forest dynamics directly.

As well, we note that these equations for terrestrial C sequestration are based on the assumption that C mineralized from SOC, biochar, or crop residue decomposition would be released in the form of CO_2 . Accounting for the possibility that some of the C is likely lost as CH_4 would increase the GHG storage value of any C remaining in these terrestrial pools. Not including loss as CH_4 results in a conservative estimation of GHG impact of the improved cook stoves.

7. Model Scenario Design

The mean values, standard deviations, and distributions of parameters described in Table 1 are based on available data and the ranges over which we expected them to vary or were interested in exploring. The MRT for passive biochar C is set so it will fall within 100 and 1000 over 95% of the time [18]. The passive biochar C fraction is set so it will fall between 0.7 and 0.9, 95% of the time, which is consistent with unpublished biochar incubation data. The fraction of maize stover gathered is set to vary uniformly between 0.25 and 0.75. This explores the effects of potential increased gathering beyond the current mean of 0.25 (which was determined through farmer surveys). The mean impact ratio of biochar on maize yields (2.16) and its standard deviation (0.69) are based on the mean response of crops with and without biochar applications in field trials on farms of

varying age categories (2 and unpublished data). The mean baseline fuel use and its standard deviation are based on data collected from the kitchen performance tests described above. The fNRB of off-farm wood is set with a mean of 0.8, based on relatively high unsustainability, but with a relatively high standard deviation of 0.25 to account for the difficulty of accurately estimating fNRB, although it cannot exceed 1 or be less than 0.

8. Model Evaluation

This model was evaluated by examining its behavior, structure, and assumptions, asking, “Is this model useful and sufficient for addressing the research question?” The model is not accepted outright as true or rejected as false, but, rather, given a series of tests to better understand its strengths and limitations and how it might be improved or expanded. In addition to the sensitivity analysis discussed in the manuscript, there were a number of tests applied that are commonly used to evaluate system dynamics models [19].

Integration error

In dynamic models that use numerical integration, the calculation interval (time step) chosen can have a significant influence on model results. If the time step is too large, the model may generate spurious oscillations. A small time step value, although it avoids the generation of spurious behaviors, may markedly increase the calculations (and time) required for a simulation. To determine a reasonable time step value, we used the test proposed by Sterman [19], which halved the value of the time step and evaluated changes in model behavior. In this case, we decreased the time step from 0.0156 months to

0.0078 months, and observed no major differences in the value or behavior for all variables.

Boundary adequacy

Tests of boundary adequacy were used to examine the impacts of assumptions about which variables are endogenous, exogenous or excluded from the model structure. The most notable boundary issues are that the effects of wood gathering on forest C stocks in both vegetation and soil are not modeled explicitly, and are instead accounted for by using the extreme case assumptions discussed in the manuscript. As indicated by the high sensitivity of the net GHG impact difference from baseline to fNRB, if we had the data to directly model the forest accurately, this could substantially improve the ability of the model to predict the effects of changes in wood-gathering behavior. This could be challenging, particularly due to the complex and heterogeneous nature of the natural forest system as well as the social and economic factors that drive wood-gathering behavior over time and industrial influences (such as the impact of harvesting wood for large-scale charcoal fuel production). The fNRB approach is common [7, 20-22] and likely a good approximation, but it would be informative and beneficial to include forest dynamics within the system boundary, were the data available.

Behavioral reproduction

This test was used to determine whether the model can generate expected behavior endogenously, and whether the model's behavior corresponds to the real-world system. As shown earlier in the SI, the behavior of the SOC passes this test. However, we note

that the modeled decline in maize stover yields is not endogenous to the model. This is acceptable, because the model is not a crop growth model, *per se*, although it uses crop growth as an input. If this model were transferred to other systems, trends in crop yields (and their response to biochar application) would have to be assessed separately.

Structure assessment

This test was used to determine whether the model conforms to basic physical laws and assumptions of human behavior. In terms of physical laws, the model appears to be robust – for example, in varying many different parameters, no physical stocks can be made negative. In terms of human behavior, the model is currently limited – *i.e.*, the decision-making processes of the actors in the model are either built into the structure (such as the decision to use fuel from sustainable sources first) or not included (family size remains constant and planted crops do not change over time). However, the model could be expanded to allow for alternative assumptions about socioeconomic decision-making.

Dimensional consistency

We ensured that the dimensions of all stocks, flows, and other parameters are consistent with reality and with each other. A units analysis using the Vensim software reveals no errors in units, but this alone is not sufficient to determine dimensional consistency. By examining each variable and asking the question, “Are these the units we would normally ascribe to this item, and do they make common sense?” we arrived at the conclusion that the model is dimensionally consistent.

Parameter assessment

This test evaluated model parameter values by asking whether they have real-world counterparts, and if they are consistent with extant knowledge about the system. Most parameters in this model are based on published or unpublished data. In general, any limitations are documented in the model. The use of a C basis for measuring fuel consumption may seem inappropriate at first glance because actors in the model would not know the C content of a given fuel, or the total C they have stored in residues, and in this model, decisions are made based on this knowledge. However, it is a reasonable assumption, because these decisions are likely to be made on an estimated mass basis, which would be directly proportional to total C content.

Extreme conditions

We examined how the model responds when certain parameter values are at minima or maxima. We varied a variety of parameters, but found no critically aberrant behavior. Its weakest point is in the human system – for example, the household size remains constant, even if crop yield declines or no wood is available, while we would expect that social changes would take place under food and fuel stress. Adding a human component to the model would be relevant, but is not critical for the questions of current interest.

9. Further GHG Impact Results

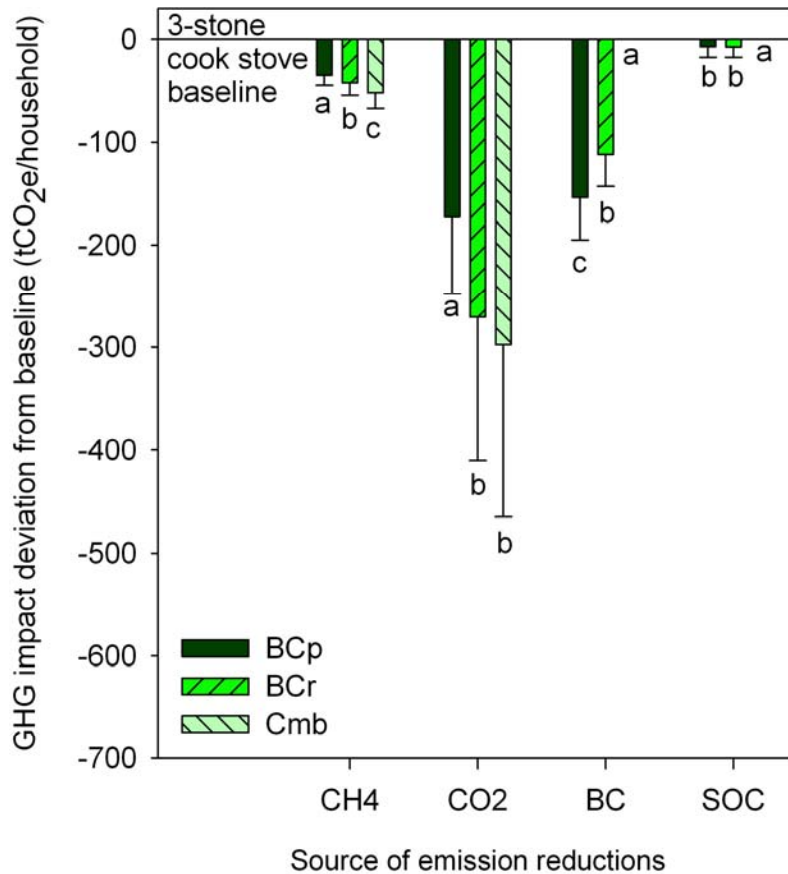


FIGURE S10. Simulated mean GHG impact deviation from baseline for each sub-component of total emissions reductions for the improved combustion stove (Cmb), the prototype biochar-producing stove (BCp), and the refined biochar-producing stove (BCr). Error bars represent standard error of 200 simulations and letters indicate significant differences within sub-components ($p < 0.05$, Tukey's HSD pairwise comparisons).

10. Further Soil Carbon Results

By drawing a wide system boundary that includes SOC on the maize fields, we see the impact of diverting crop residues from the fields to stove uses. The total SOC losses predicted in this model under 3-stone stove conditions for a newly converted farm are around 40 tC/ha over 100 years, which is consistent with global SOC loss rates in agricultural soils [23]. The production of biochar and its addition to soils increases the

amount of non-biochar soil C because it increases crop yields, thus enhancing net stover return to the soil (Figure S11).

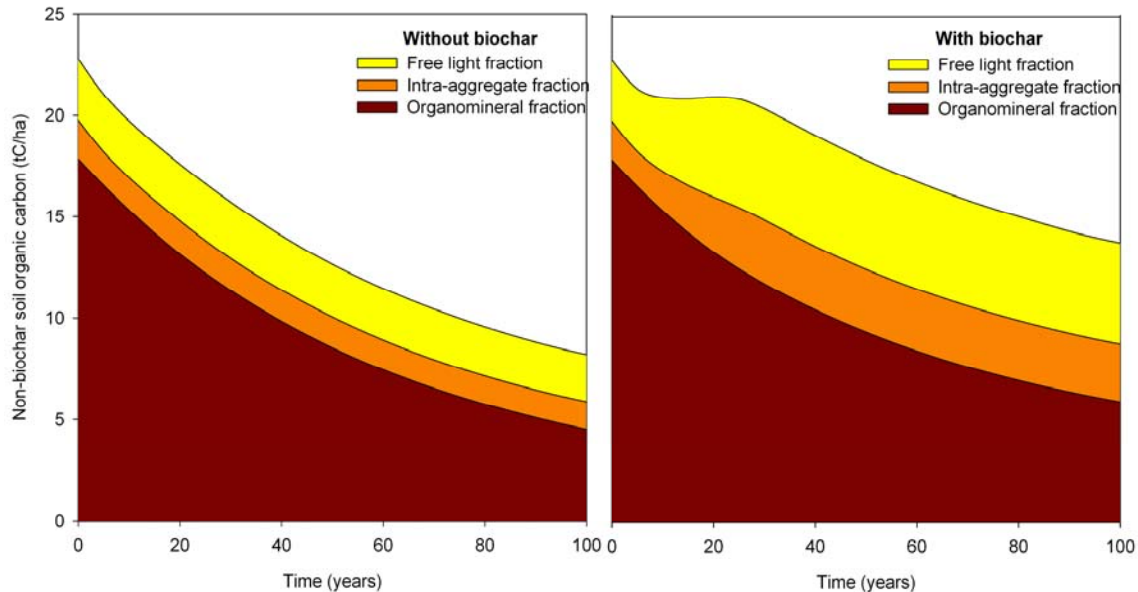


FIGURE S11. Simulated non-biochar soil organic C stocks over 100 years under a 3-stone cook stove (left) and the prototype biochar-producing cook stove (right). Model settings are those used as default in the main manuscript – i.e., a 30-year old farm, which has already experienced soil C depletion.

As discussed in the main manuscript, increasing the gathering of stover could help provide a renewable source of biomass fuel, which could replace other biomass fuel sources. As well as being a climate change-related choice, the amount of stover to gather for fuel use is also an economic and agronomic choice, as increased use of corn stover for fuel could divert it from other uses, such as animal feed, or from the important role it plays protecting the soil [24]. If residue gathering were increased from 25% to 50%, this would initially deplete non-biochar SOC stocks, but as applied biochar increases crop yields, stover inputs increase to make up for this deficit (Figure S12). Under the baseline model scenario described in the paper, the losses of soil C due to increased harvesting are

not fully offset by increased crop growth until 15-20 years after the stove is introduced. This highlights the importance of the temporal dynamics that system dynamics modeling can allow us to examine quantitatively.

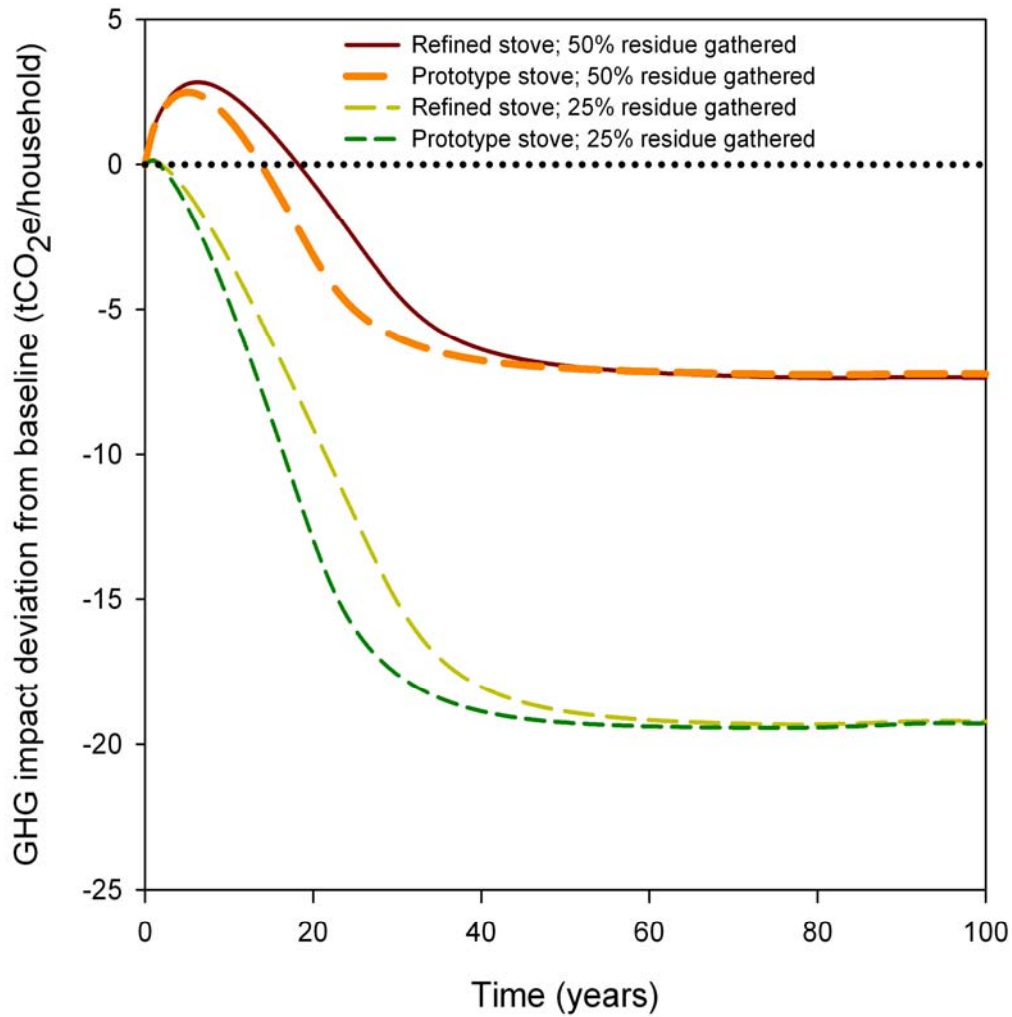


FIGURE S12. Simulated non-biochar soil C GHG impact deviation from baseline for biochar producing stoves under 25% and 50% residue-gathering regimes over time.

11. Further Sensitivity Analysis Results

Varying time since farm conversion from forest or soil fertility status has a relatively small effect on the GHG impact (Figure S13). Thus, having a wide range of farm ages or soil fertility statuses in a given project may not be a significant issue. While the farm age is primarily important for determining SOC stocks and the effect of biochar application on maize growth, changes in initial SOC stocks are not very influential for the net GHG impact.

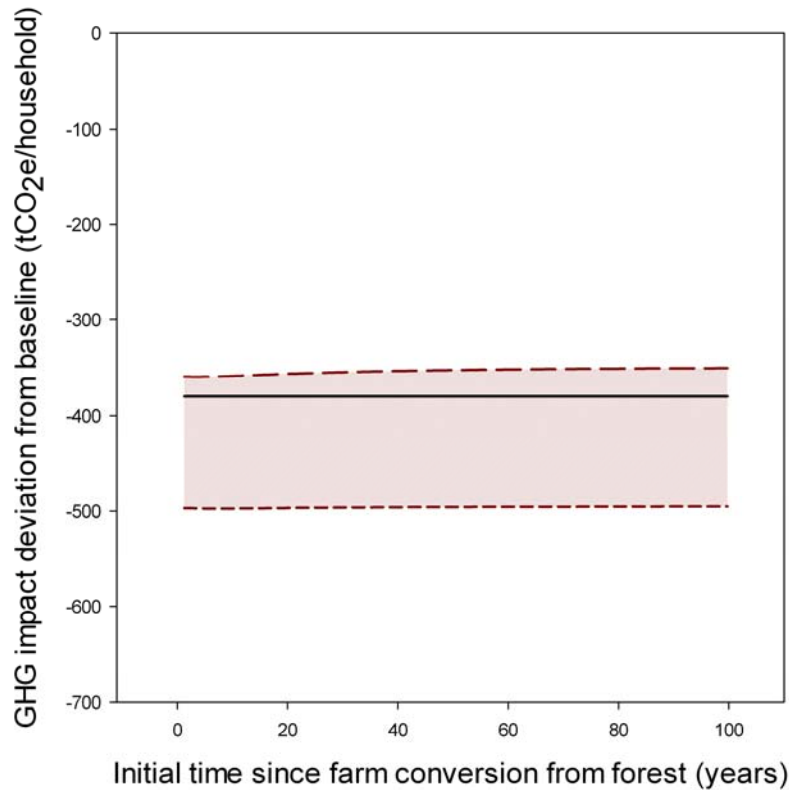


FIGURE S13. Simulated sensitivity of calculated GHG impact deviation from 3-stone stove baseline after 100 years when initial farm age is varied between 1 year and 100 years. The prototype pyrolysis stove is represented by the long dashed line, the refined pyrolysis stove by the short dashed line, and the improved combustion stove by the solid line. The shaded area highlights the range between the mean values of the two pyrolysis stoves. More negative values indicate greater GHG reductions.

12. Policy Analysis Results

The inclusion of non-Kyoto-regulated CO gas and particulate black C (Figure S14A) increases the net GHG impact reductions from the baseline scenario by 7.5% for the refined pyrolysis cook stove, 7.3% for the prototype biochar cook stove, and by 10.1% for the improved combustion cook stove. Their inclusion accentuates the importance of the gaseous emissions and those factors that affect the accounting of emissions, such as the fNRB. Even though the CO:CO₂ ratio is higher for the pyrolysis stoves than for the improved combustion cook stove (Table S2), which would increase the effect of including non-Kyoto gases, gaseous emissions make up a greater fraction (100%) of the net reductions from baseline for the improved combustion stove. Therefore, including non-Kyoto gases increases the GHG impact reduction more for the improved combustion cook stove than for both pyrolysis cook stoves.

When biochar that was produced from unsustainably harvested woody biomass is counted as an effective instant emission, rather than a neutral change in C stocks (Figure S14B), the net GHG impact reduction from the baseline scenario decreases by 0.2% for the refined pyrolysis cook stove and by 1.7% for the prototype pyrolysis cook stove.

Although there is no net change in terrestrial C stocks when biochar is produced from unsustainably harvested wood, as the system is defined here, there could be other reasons that one would choose to value either C in the form of a living forest or C in the form of biochar for soil improvement over the other. An NGO focused on forest preservation might choose to value standing forests, whereas a farmer might not place the same value on intact forests as on cleared forests for agriculture, combined with biochar production

for soil application that results in more productive soils. This decision might be made when applying C accounting protocols to a biochar system in order to ensure that an incentive for deforestation is not inadvertently created. Although the biochar stove modeled here uses less wood than the baseline scenario's 3-stone stove, one can imagine a scenario where a stove that uses more wood in total, but produces enough biochar, could mask the effect of increased deforestation, since biochar production is counted as no net change. Thus, we have not made a value judgement in this model, but draw attention to this choice. Because the impact of this policy choice on the net reductions is relatively low, even at maximum fNRB, it may be possible to err on the side of forest preservation by counting biochar production from unsustainably gathered biomass as an immediate emission.

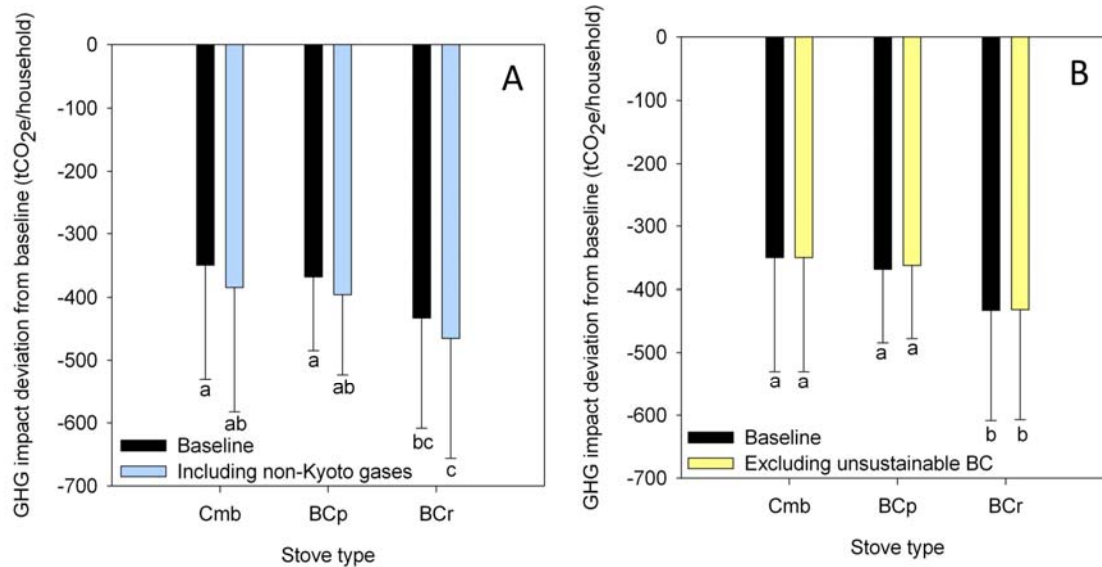


FIGURE S14. Simulated influence of policy choices on mean GHG impact deviation from baseline after 100 years. Error bars represent standard error over 200 simulations. Results are shown for the refined biochar-producing cook stove (BCr), the prototype biochar-producing cook stove (BCp), and the improved combustion cook stove (Cmb). Letters indicate significant differences between stoves and scenarios for each policy choice ($p < 0.05$, Tukey's HSD pairwise comparisons). A - Non-Kyoto gases are included or excluded from the GHG accounting of the system. B - Biochar produced from unsustainably harvested wood is considered to be neutral as long as it remains stable or is treated as a net loss of C to the atmosphere upon conversion.

13. Literature Cited

1. Ngoze, S.; Riha, S.; Lehmann, J.; Verchot, L.; Kinyangi, J.; Mbugua, D.; Pell, A. Nutrient constraints to tropical agroecosystem productivity in long-term degrading soils. *Glob. Change Biol.* **2008**, *14* (12), 2810-2822; DOI 10.1111/j.1365-2486.2008.01698.x.
2. Kimetu, J. M.; Lehmann, J.; Ngoze, S. O.; Mugendi, D. N.; Kinyangi, J. M.; Riha, S.; Verchot, L.; Recha, J. W.; Pell, A. N. Reversibility of soil productivity decline with organic matter of differing quality along a degradation gradient. *Ecosystems* **2008**, *11* (5), 726-739; DOI 10.1007/s10021-008-9154-z.
3. Kinyangi, J. M. Soil degradation, thresholds, and dynamics of long-term cultivation: from landscape biogeochemistry to nanoscale biogeocomplexity. PhD Dissertation, Cornell University, Ithaca, NY, 2008.
4. Tittonell, P.; Vanlauwe, B.; de Ridder, N.; Giller, K. E. Heterogeneity of crop productivity and resource use efficiency within smallholder Kenyan farms: Soil fertility gradients or management intensity gradients? *Agr. Syst.* **2007**, *94* (2), 376-390; DOI 10.1016/j.agsy.2006.10.012.
5. Torres, D. Biochar production with pyrolysis cook stoves and use as a soil conditioner in western Kenya. Master's Thesis, Cornell University, Ithaca, NY, 2010.
6. *Kitchen Performance Test (KPT), Version 3.0*; Bailis, R.; Smith, K.; Edwards, R.; Household Energy and Health Programme, Shell Foundation: 2007; http://ehs.sph.berkeley.edu/hem/content/KPT_Version_3.0_Jan2007a.pdf.
7. MacCarty, N.; Ogle, D.; Still, D.; Bond, T.; Roden, C. A laboratory comparison of the global warming impact of five major types of biomass cooking stoves. *Energ. Sust. Dev.* **2008**, *12* (2), 5-14.
8. Jetter, J. J.; Kariher, P. Solid-fuel household cook stoves: Characterization of performance and emissions. *Biomass Bioenerg.* **2009**, *33* (2), 294-305; DOI 10.1016/j.agsy.2006.10.012.
9. Johnson, M.; Edwards, R.; Frenk, C. A.; Maser, O. In-field greenhouse gas emissions from cookstoves in rural Mexican households. *Atmos. Environ.* **2008**, *42* (6), 1206-1222; DOI 10.1016/j.atmosenv.2007.10.034.
10. Smith, K.R. Health, energy, and greenhouse-gas impacts of biomass combustion in household stoves. *Energ. Sust. Dev.* **1994**, *1* (4), 23-29.
11. Wang, S.; Wei, W.; Du, L.; Li, G.; Hao, J. Characteristics of gaseous pollutants from biofuel-stoves in rural China. *Atmos. Environ.* **2009**, *43* (27), 4148-4154; DOI 10.1016/j.atmosenv.2009.05.040.
12. Roden, C. A.; Bond, T. C.; Conway, S.; Benjamin, A.; Pinel, O. Emission factors and real-time optical properties of particles emitted from traditional wood burning cookstoves. *Environ. Sci. Technol.* **2006**, *40* (21), 6750-6757; DOI 10.1021/es052080i.
13. Forster, P. et al. Changes in Atmospheric Constituents and in Radiative Forcing. In *Climate Change 2007: The Physical Science Basis. Contribution of Working Group I to the Fourth Assessment Report of the Intergovernmental Panel on Climate Change*, Solomon, S.; Qin, D.; Manning, M.; Chen, Z.; Marquis, M.; Averyt, K. B.; Tignor, M.; Miller, H. L., Eds. Cambridge University Press: Cambridge, United Kingdom and New York, NY, USA 2007; pp 129.

14. Reddy, M. S.; Boucher, O. Climate impact of black carbon emitted from energy consumption in the world's regions. *Geophys. Res. Lett.* **2007**, *34* (11), L11802; DOI 10.1029/2006gl028904.
15. Bond, T. C.; Sun, H. L. Can reducing black carbon emissions counteract global warming? *Environ. Sci. Technol.* **2005**, *39* (16), 5921-5926; DOI 10.1021/es0480421.
16. Rypdal, K.; Rive, N.; Berntsen, T. K.; Klimont, Z.; Mideksa, T. K.; Myhre, G.; Skeie, R. B. Costs and global impacts of black carbon abatement strategies. *Tellus B* **2009**, *61* (4), 625-641; DOI 10.1111/j.1600-0889.2009.00430.x.
17. Bond, T. C.; Streets, D. G.; Yarber, K. F.; Nelson, S. M.; Woo, J. H. Klimont, Z., A technology-based global inventory of black and organic carbon emissions from combustion. *J. Geophys. Res.-Atmos.* **2004**, *109* (D14), 43; DOI 10.1029/2003jd003697.
18. Cheng, C.-H.; Lehmann, J.; Thies, J.E.; Burton, S.D. Stability of black carbon in soils across a climatic gradient. *J. Geophys. Res.* **2008**, *11*, G02027; DOI 10.1029/2007jg000642.
19. Sterman, J., *Business dynamics : systems thinking and modeling for a complex world*; Irwin/McGraw-Hill: Boston, 2000.
20. Johnson, M.; Edwards, R.; Ghilardi, A.; Berrueta, V.; Gillen, D.; Frenk, C. A.; Masera, O. Quantification of carbon savings from improved biomass cookstove projects. *Environ. Sci. Technol.* **2009**, *43* (7), 2456-2462; DOI 10.1021/es801564u.
21. *Energy Efficiency Measures in Thermal Applications of Non-Renewable Biomass*; CDM Executive Board; United Nations Framework Convention on Climate Change: Bonn, 2009;
<http://cdm.unfccc.int/methodologies/DB/HVLUZ94B86UAM25MUWSLT2O98PBVAR>.
22. *Indicative Programme, Baseline, and Monitoring Methodology for Improved Cook-Stoves and Kitchen Regimes*; Gold Standard: Geneva, Switzerland, 2010;
http://www.cdmgoldstandard.org/fileadmin/editors/files/6_GS_technical_docs/manuals_and_methodologies/GS_Methodology_Cookstove.pdf.
23. Lal, R.; Follett, F.; Stewart, B. A.; Kimble, J. M. Soil carbon sequestration to mitigate climate change and advance food security. *Soil Sci.* **2007**, *172* (12), 943-956; DOI 10.1097/ss.0b013e31815cc498.
24. Lal, R. Challenges and opportunities in soil organic matter research. *Eur. J. Soil Sci.* **2009**, *60* (2), 158-169; DOI 10.1111/j.1365-2389.2008.01114.x.